A. González-Cantos
A. Ollero
Grupo de Robótica, Visión y Control
Departamento de Ingeniería de Sistemas y Automática
Camino de los Descubrimientos, s/n, 41092 Sevilla, Spain
alberto.gonzalez@uca.es

Backing-Up Maneuvers of Autonomous Tractor-Trailer Vehicles using the Qualitative Theory of Nonlinear Dynamical Systems

Abstract

This paper presents an approach, based on the qualitative theory of nonlinear dynamical systems, for the analysis and design of control systems for autonomous articulated vehicles. In particular, backing-up maneuvers are considered. These maneuvers are dangerous because the vehicles tend to 'jackknife' when the angle between the tractor and the trailer is greater than a certain value. This danger is increased when the actuators are saturated because they can cause a lack of controllability in the state space and control becomes complicated. The paper proposes a two-level control system with an orientation controller in the lower level and a look-ahead controller in the higher. In the paper, a general orientation feedback controller is presented. This control strategy represents a wide family of different nonlinear controllers and can be applied with different particular control laws. The paper applies the qualitative theory of nonlinear dynamical systems to study the stability of the control system. Thus, the stability of the system under some constraints is demonstrated. The paper includes both simulation and experimental results of the implementation on the Romeo 4R autonomous vehicle, which is a full-size autonomous electrical golf cart with a trailer.

KEY WORDS—Autonomous articulated, vehicles, backing-up maneuvers, nonlinear dynamical systems

1. Introduction

Articulated vehicles have a pivoting joint which allows the vehicle to turn more sharply. They can be used to transport goods or people in cluttered environments that cannot be navigated by vehicles with only one rigid body because the turning radii of the articulated vehicles are significantly shorter. Moreover, articulated vehicles are useful when the floor is uneven and irregular because the articulation makes it possible for the driving wheels to maintain contact with the floor. This paper deals with autonomous articulated vehicles in which the joint is not actuated. These vehicles are usually called tractor-trailers or truck-trailers. It has been shown that the forward motion of tractor-trailers is naturally stable because the trailer tends to align with the truck without any control action (Gonzalez-Cantos et al. 2001). However, this is not the case with the backing-up maneuvers considered in this paper. These maneuvers are required in many loading and transportation tasks in industrial and urban environments because they drastically decrease the space required to position the vehicle in the loading stations, park in a given urban parking place or navigate through way-points in cluttered industrial environments.

Backward steering control of autonomous articulated vehicles has been the subject of several papers (see, for example, DeSantis 1994; Sampei et al. 1995; Lamiraux and Laumond 1998; Kim and Oh 1999; Li et al. 1999; Nakamura et al. 2000) and some of them present results of the implementation in specially built laboratory mobile robots. Fuzzy control, neural networks and genetic algorithms have also been applied to the backward steering of truck-trailers. Some of these papers deal with stability and robustness issues. Some authors (Tokunaga and Ichihashi 1992; Tanaka and Sano 1994) have therefore presented designs for fuzzy controllers such that the control system is asymptotically stable in all the state space. However, these results are based on the assumption that the values of the angle between the longitudinal axis of the tractor and the trailer are small. This assumption is realistic in many

The International Journal of Robotics Research
Vol. 28, No. 1, January 2009, pp. 49–65
DOI: 10.1177/0278364908097588

Figures 13, 16–18 appear in color online: http://ijr.sagepub.com

trajectory tracking and lateral vehicle control problems in open fields or autonomous driving in roads. However, the assumption is not realistic when maneuvering in constrained spaces, such as those encountered in industrial environments for example. These maneuvers are particularly dangerous because the vehicle can 'jackknife' when the angle between the tractor and the trailer is greater than a certain value, possibly destroying the roller in the joint between the tractor and the trailer.

Furthermore, De Luca et al. (1998) and Lamiraux et al. (1999) have presented several successful feedback solutions for point stabilization, path following and trajectory tracking control tasks executed by a mobile robot with car-like kinematics, and have demonstrated the stability of the proposed solutions. These results are based on the assumption that there is no actuator saturation.

This paper proposes a control system without the small-angle assumption mentioned above. The design approach is based on the results presented in González-Cantos et al. (2001). Furthermore, actuator saturation is considered here. Actuator saturation complicates the control because it can cause a lack of controllability in the state space, as will be shown.

In Astolfi et al. (2004) the path tracking of a tractor trailer for straight and circular forward/backward motions is addressed using Lyapunov techniques. The method is based on the direct decrease in the tractor lateral offset and orientation offset with respect to the path. The saturation of the steering actuation is considered and the stability is demonstrated. The control law proposed in this paper is obtained for circular and rectilinear paths. Furthermore, there is no analytic expression for the control law, so it has to be obtained by numerical integration. The control strategies are only tested in simulation.

In this paper, a different method for steering the truck-trailer for path tracking in backing-up maneuvers is considered. The paper proposes a general orientation feedback control that can be particularized for different nonlinear control laws. The steering for tracking the path is based on the look-ahead approach, which is possibly one of the most efficient, practical methods for path tracking of real autonomous vehicles. This approach consists of steering the vehicle toward a target point on the path to be tracked. The most critical point in the look-ahead approach is the selection of the target point at each moment of the process. Thus, the paper explicitly relates the look-ahead point to the stability of the closed loop controller by using the qualitative theory of nonlinear dynamical systems. The method has been applied to steering the Romeo 4R (a full size golf-cart vehicle) backwards at significant speeds. This tractor-trailer vehicle is being used as a test-bed in the framework of the CROMAT (Coordination of aerial and ground robots (in Spanish)) and AEROSENS (Aerial robots and sensor networks with mobile nodes for cooperative perception (in Spanish)) projects for the coordination of autonomous aerial and ground vehicles.

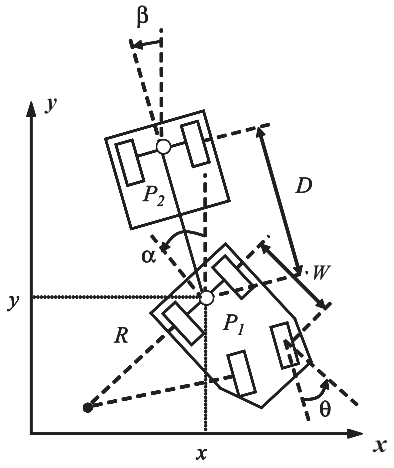

Fig. 1. Articulated vehicles.

The paper is organized as follows. First, the adopted model of the tractor-trailer system is presented and the backing-up control problem is stated by including the controllability study and the proposed control structure, which is based on two control levels: orientation control and look-ahead control. The following two sections present the analysis and design techniques involved in each of these two levels. A section is then devoted to the experiments with the Romeo 4R.

2. Model

The study of the motion of a vehicle, including kinematics and dynamic equations, vehicle/terrain interaction, actuator dynamics, etc. is very complex. Thus, certain acceptable approximations are made for the analysis. It is usually assumed that the wheels do not slip. The deformation of the tires is also ignored for the sake of simplicity. These assumptions are acceptable for vehicles moving at low speeds over compact terrains. Furthermore, the analysis is performed for the planar motion of a vehicle on a horizontal plane. Thus, as a first approximation, a simplified two-dimensional (2D) model is considered, with the assumption that the vehicle moves in a plane. Moreover, for vehicles moving at low speed, the actuator dynamics can be neglected. Further considerations of this dynamic behavior will be discussed in Section 6 of the paper.

Consider the vehicle illustrated in Figure 1 where (x, y) are Cartesian coordinates; P_1 and P_2 are the middle points of the tractor and trailer rear wheels, respectively; W is the distance between the front and rear axis of the tractor; D is the distance between the middle points of the rear axis of the tractor and the axis of the trailer (see Figure 1); α and β are the tractor's orientation and the trailer's orientation, respectively; θ is the steering angle and R is the curvature radius at the guidance point of the tractor on the tractor's path. Notice that in this paper we consider the case in which the joint linking the

trailer to the tractor is located at the midpoint of the tractor's rear axis (on-axle hitching model). This is a common assumption (e.g. Kong and Kosko 1992; Sampei et al. 1995; Samson 1995; Tanaka et al. 1997) that makes the control problem easier to tackle (Bolzern and Locatelli 2002). Using the kinematics model for the system in Figure 1, the following expression can be obtained:

$$\begin{pmatrix} \dot{x} \\ \dot{y} \\ \dot{\alpha} \\ \dot{\beta} \end{pmatrix} = \begin{pmatrix} -\cos(\beta-\alpha)\sin\beta & 0 \\ \cos(\beta-\alpha)\cos\beta & 0 \\ 0 & -1 \\ \dfrac{\sin(\beta-\alpha)}{D} & 0 \end{pmatrix} \begin{pmatrix} v \\ vu \end{pmatrix} \quad (1)$$

where (x, y) are Cartesian coordinates of P_2, v is the backing-up speed and $u = 1/R = \tan(\theta)/W$ is the curvature of the tractor that will be used as the control action.

We will focus on the steering control, or lateral control, to track a given path. Thus, the velocity v will be considered constant. However, it should be noted that the velocity is related to the longitudinal control, which can be implemented by means of a simple PID (Proportional Integral and Derivative) controller.

If a new timescale $\tau = vt$ is defined, Equations (1) can be written:

$$\begin{pmatrix} \dfrac{dx}{d\tau} \\ \dfrac{dy}{d\tau} \\ \dfrac{d\alpha}{d\tau} \\ \dfrac{d\beta}{d\tau} \end{pmatrix} = \begin{pmatrix} -\cos(\beta-\alpha)\sin\beta & 0 \\ \cos(\beta-\alpha)\cos\beta & 0 \\ 0 & -1 \\ \dfrac{\sin(\beta-\alpha)}{D} & 0 \end{pmatrix} \begin{pmatrix} 1 \\ u \end{pmatrix} \quad (2)$$

where $v = 1$ is assumed without any lack of generality.

It is also assumed, without loss of generality, that the trailer jackknifes when $|\beta - \alpha| = \pi/2$. In practice, the exact jackknife angle depends on the particular characteristics of the vehicle. The results presented below can be applied for any value of the angle $|\beta - \alpha|$ without additional considerations. Other kinematics singularities such as $|\beta - \alpha| = \pi$ are not considered in this analysis because they do not correspond to real situations; the angle in the joint cannot reach these values without jackknifing first.

3. Backing-Up Control

In this section, the Controllability Minimum Principle (Thomas and Walter 1997) is used to show that the controllable set of the system is not all state space when the saturation in the actuators is considered.

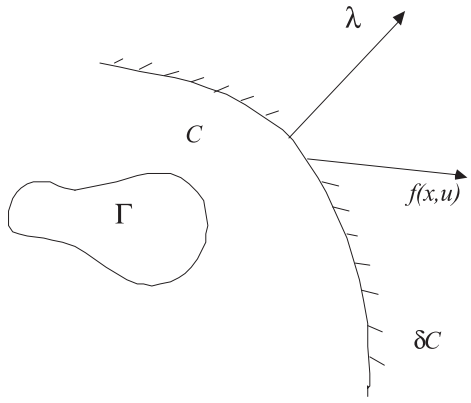

Fig. 2. Controllable set.

Controllability Minimum Principle: *Let u(x) be an admissible control law that generates a trajectory x(t) that satisfies*

$$\dot{x} = f(x, u(x)) \quad u(x) \in U \quad (3)$$

with x(t) lying in the boundary δC of the controllable set C to Γ *(the set of states that can be driven to* Γ *through an admissible input) for some interval* $0 \le t \le t_f$. *Then there exists a non-zero continuous* n_x*-dimensional outward normal vector* $\lambda(t)$ *to δC such that, for all* $t \in (0, t_f)$,

$$\begin{aligned} 0 &= H(x(t), u[x(t)], \lambda(t)) \\ &= \min_{u \in U} H[x(t), u, \lambda(t)] \end{aligned} \quad (4)$$

with $\lambda(t)$ *satisfying*

$$\dot{\lambda}^T = -\frac{\partial H}{\partial x} - \frac{\partial H}{\partial u}\frac{\partial u}{\partial x} \quad (5)$$

where $H(x, u, \lambda) = \lambda^T f(x, u)$ (see Figure 2).

As a result of this principle, the boundary δC of the controllable set C forms a separating surface in the state space, i.e. a semi-permeable membrane. Thus, there is no admissible control law $u(x)$ that could lead the state of the system to cross this surface from the outside of C to the inside, but it is possible for the state of the system to cross the surface from the inside of C to the outside.

Taking into account the above principle and considering the saturation of the actuator $|u| \le U_{\text{sat}}$, it is possible to show that if the maximum curvature of the tractor U_{sat} is smaller than $1/D$, the controllable set to the region $\Theta = \{(x, y, \alpha, \beta) \,||\sin(\beta - \alpha)| \le DU_{\text{sat}}\}$ is Θ. In this case, the boundaries δC of the controllable set are defined by the lines $\beta - \alpha = \pm \arcsin(DU_{\text{sat}})$ (see Figure 3). Thus, if the system crosses to the outside of Θ, there is no admissible control law that carries back the system to the inside of Θ and therefore the

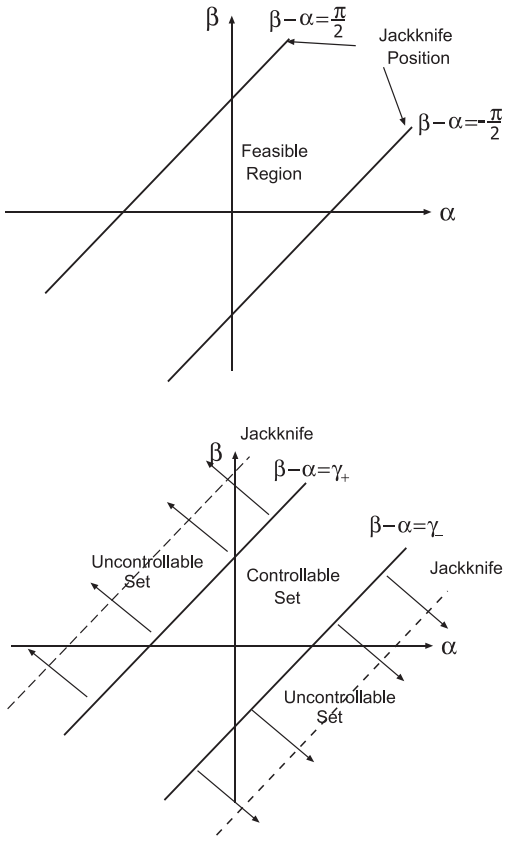

Fig. 3. Controllable set with $DU_{\text{sat}} \geq 1$ (upper) and $DU_{\text{sat}} < 1$ (lower). Note that in the second case, Θ is smaller. The values of γ_+ and γ_- are given by $\gamma_\pm = \pm \arcsin(DU_{\text{sat}})$.

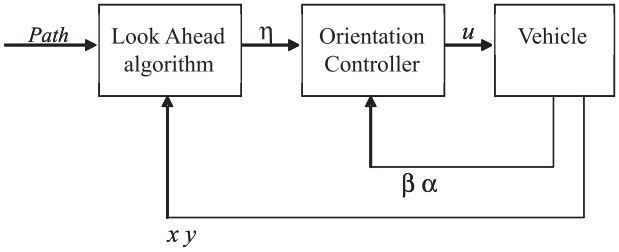

Fig. 4. Controller's levels.

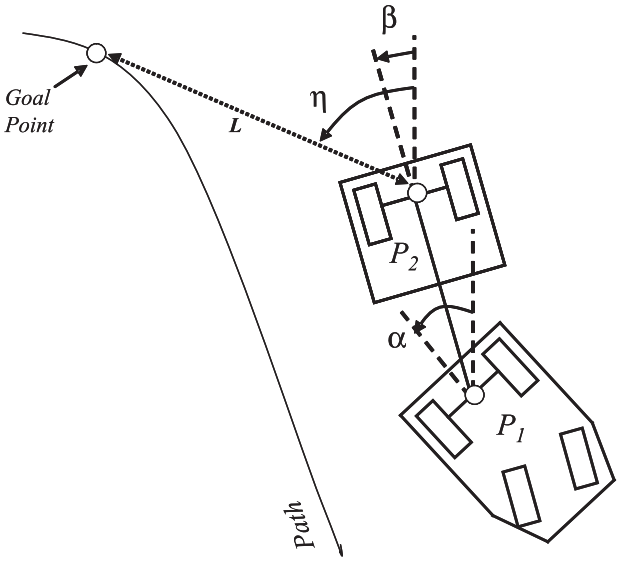

Fig. 5. Look-ahead algorithm.

system will reach the jackknife position. Thus, the constraints on the angle $\gamma = \beta - \alpha$ between the tractor's orientation with respect to the trailer's orientation can be expressed as:

- if $DU_{\text{sat}} \geq 1$ then $|\gamma| \leq \pi/2$; or
- if $DU_{\text{sat}} < 1$ then $|\gamma| \leq \arcsin(DU_{\text{sat}})$

where the first condition is obtained from the physical limits of the jackknife condition defined in Section 2 and the second from the definition of Θ. The above constraints should be maintained by the control system in order to avoid losing control and reaching the jackknife position. Figure 3 shows the different controllable sets depending on the above conditions.

By applying the controllability minimum principle, it can be shown that if the actuator dynamic is taken into account, the controllable set is reduced. Furthermore, if the system goes out to the controllable set, it is necessary to drive forward to realign the truck-trailer in order to avoid jackknifing. In Altafini et al. (2001), a hybrid control system based on this idea is presented. It should be noted that the switching surfaces can be lines $\beta - \alpha = \gamma_\pm$ (with hysteresis).

The control system proposed in this paper is based on a two-level hierarchical structure. The upper level or *look-ahead level* consists of the outer loop in Figure 4. The aim of this level is to track a given path defined by the maneuver. Thus, it is based on the computation of the error between the vehicle and a goal point selected on the path at a given look-ahead distance L; that is, the so-called pure pursuit strategy (Amidi 1990) is applied. The controller at this level computes the orientation angle η of the line defined by the middle points of the tractor's rear axis and the goal point (see Figure 5). This orientation angle will be the reference for the second level.

The lower level is the *orientation controller*, defined by the inner loop in Figure 3. This level generates the control u of the vehicle's steering actuator so that the vehicle reaches the desired orientation η provided by the higher level controller in the outer loop. As a first analysis, it is possible to consider a system with dynamics of two different timescales: the look-ahead controller with a slow dynamics and the orientation controller with a faster dynamics.

4. Orientation Controller Design

The objective of this level is that the vehicle follows the desired orientation η, while avoiding the loss of control and the jack-knife position. Therefore, this controller should control both the tractor's orientation α and the trailer's orientation β at the same time, in order to reach the desired orientation η.

The following general controller is proposed:

$$u(t) = \Psi(\gamma)_1 (\alpha - \eta) + \Psi(\gamma)_2 (\beta - \eta) \tag{6}$$

where $\gamma = \beta - \alpha$ and Ψ_1, Ψ_2 are functions that satisfy the following conditions:

- Ψ_1, Ψ_2 are functions of Class C^1;
- $\Psi_1 > 0, \Psi_2 < 0$ and $|\Psi_2| \geq \Psi_1 > \dfrac{1}{D}$;
- $\Psi\left(\pm\gamma_{\max}\right)_1 = -\Psi\left(\pm\gamma_{\max}\right)_2$;
- $\Psi(\gamma)_{1,2} = \Psi(-\gamma)_{1,2}$.

Note that this general controller represents a wide family of different nonlinear controllers. Here, we undertake a general stability analysis to provide the stability conditions of the general controller Equation (6) without regard to particular design techniques.

From Equation (2), the dynamic behavior at this level is:

$$\begin{pmatrix} \dfrac{d\alpha}{d\tau} \\ \dfrac{d\beta}{d\tau} \end{pmatrix} = \begin{pmatrix} \Phi(\Psi_1(\eta - \alpha) + \Psi_2(\eta - \beta)) \\ \dfrac{\sin\gamma}{D} \end{pmatrix} \tag{7}$$

where $\Phi(s)$ denotes a saturation function $\Phi : R \rightarrow R$. If $u_{\max} \in R$ with $u_{\max} > 0$ then:

- if $\|s\| \leq u_{\max}$ then $\Phi(s) = s$;
- if $s > u_{\max}$ then $\Phi(s) = u_{\max}$; or
- if $s < u_{\max}$ then $\Phi(s) = -u_{\max}$.

The aim of this section is to study the stability of Equation (7) depending on the values of the functions Ψ_1, Ψ_2; that is, to determine which additional conditions have to satisfy the functions Ψ_1, Ψ_2 in order to guarantee the stability and to reach the desired orientation.

In practice, the desired path should be smooth enough that the dynamics of the desired orientation η should be slower than the dynamics of α and β.

Here, stability constraints on the shape of the functions Ψ_1, Ψ_2 will be given. We will assume that η is constant. Without lack of generality in the analysis, $\eta = 0$.

Consider the following quadratic Lyapunov function:

$$V = (\alpha, \beta)^T \begin{pmatrix} 1 & b \\ b & a \end{pmatrix} (\alpha, \beta) > 0 \tag{8}$$

where

$$a = \frac{\Delta(1 - b) + \min\Psi_2 D(b + 1)}{\Delta}$$

$$\text{and} \quad b = \frac{\min\Psi_2}{\min\Psi_1} \tag{9}$$

and $\Delta = \sin\gamma_{\max}/\gamma_{\max}$. It is possible to show that $\dot{V} < 0$ if the following conditions are satisfied:

- $\Psi_1 > -\frac{\Delta}{D} b, \forall\gamma$
- $-1 > b > -2$ (10)
- $\left|\frac{d\Psi_1}{d\gamma}\right| \geq p(\gamma) \left|\frac{d\Psi_2}{d\gamma}\right| \geq 0, \forall\gamma$

where $0 \leq p < b + 2, \forall\gamma$.

The system is therefore stable without actuator saturation if the above conditions are satisfied. In the case of saturation in the actuator, additional analysis is necessary. Here we will show how this stability can be guaranteed even when the controllable set is not all state space under the condition $DU_{\text{sat}} < 1$ in Section 3 above. Let S^1 be the positive saturation set, S^{-1} the negative saturation set and S^0 the non-saturation set, defined as:

$$S^1 = \{\alpha, \beta / \Psi_1\alpha + \Psi_2\beta \geq U_{\text{sat}}\} \tag{11}$$

$$S^{-1} = \{\alpha, \beta / \Psi_1\alpha + \Psi_2\beta \leq -U_{\text{sat}}\} \tag{12}$$

$$S^0 = \left\{\alpha, \beta \in \Re^2 \cap S^1 \cap S^{-1}\right\}. \tag{13}$$

Proposition 1: *Let $\phi(t)$ be any trajectory of Equation (6) where $\phi(0) \in S^1$. Then there exists a time $t_a > 0$ at which $\phi(t_a) \in S^0$.*

Proof: The proof will be divided in two cases.

1. Assume that $\alpha < 0$ and $\gamma > 0$. Since the system is in S^1, $\dot{\alpha} < 0$, $\dot{\gamma} > 0$ and it will remain as such until it goes out of S^1. Furthermore, as $\Psi_1 > 0$ and $\Psi_2 < 0$, $\alpha < \beta < 0$. On the other hand, consider the parameter ε defined as follows:
$$\varepsilon = U_{\text{sat}} - \Psi_1\alpha - \Psi_2\beta \tag{14}$$
where $\varepsilon < 0$ if $(\alpha, \beta) \in S^1$. By differentiating with respect to time,
$$\dot{\varepsilon} = -\left(\frac{d\Psi_1}{d\gamma}\alpha + \frac{d\Psi_2}{d\gamma}\beta\right)\dot{\gamma} - \Psi_1\dot{\alpha} - \Psi_1\dot{\beta}. \tag{15}$$
Taking into account the above conditions of the functions Ψ_1, Ψ_2, the following inequality is satisfied:
$$\dot{\varepsilon} > U_{\text{sat}}\left(\Psi_1 - \frac{d\Psi_1}{d\gamma}\alpha(1 - p)\right) - \frac{\sin\gamma}{D}\left(\Psi_2 + \frac{d\Psi_1}{d\gamma}\alpha(1 - p)\right). \tag{16}$$

Thus $\dot{\varepsilon} > 0$. However, there exists a time $t_a > 0$ at which $\varepsilon > 0$; thus, the system enters into S^0.

2. Assume that the system does not correspond to the conditions assumed for case (1), since $\dot{\alpha} < 0$ and $\dot{\gamma} > 0$. In this case, the evolution of the system has two possibilities: it can enter into S^0 or it can remain in S^1 until it has the conditions for case (1), at which time the system will go out of S^1. Similar reasoning can be carried out if $\phi(0) \in S^{-1}$.

Taking into account Proposition 1 and the fact that $\dot{V} < 0$, it is possible to confirm that the origin is stable in the controllable set unless there is a limit-cycle. In Appendix A we show that Equation (7) does not have a limit cycle. Thus, stability in the controllable set is assured with the proposed control structure.

Furthermore, as $\Psi\left(\pm\gamma_{\max}\right)_1 = -\Psi\left(\pm\gamma_{\max}\right)_2$, the following conditions are satisfied:

$$\left.\frac{d\gamma}{dt}\right|_{\gamma\ \min} > 0, \quad \left.\frac{d\gamma}{dt}\right|_{\gamma\ \max} < 0. \tag{17}$$

Thus, the system does not leave the controllable set and jackknifing is avoided. In summary, the conditions for achieving stability, even when the actuator saturation is taken into account, and when the controllable set is not all state-space, have been presented above.

This analysis can be applied to a wide family of controllers defined by Equation (6). Thus, a nonlinear controller and fuzzy controller have been simulated to show the stability results of this analysis. The proposed nonlinear controller is given by:

$$\begin{aligned} u(t) &= (k_{11} - k_{12}\cos(\gamma))\,\alpha(t) \\ &+ (k_{21} - k_{22}\cos(\gamma))\,\beta(t). \end{aligned} \tag{18}$$

This controller is a particular case for the family of Equation (6).

For the fuzzy controller, the structure proposed in Gonzalez-Cantos et al. (2001) is used. It is based on the following rules.

Rule 1: IF γ is C_i THEN $u(t) = f_i(\alpha, \beta)$

where $f_i(\alpha, \beta) = k_{i1}\alpha + k_{i2}\beta$, C_i is defined by means of a membership function $\omega_i(\gamma)$, and k_{i1} and k_{i2} are constants. Thus, the controller can be expressed as

$$\begin{aligned} \Psi(\gamma)_1 &= \left(\sum_{i=1}^{n} i\omega(\gamma)\,k_{i1}\right), \\ \Psi(\gamma)_2 &= \left(\sum_{i=1}^{n} i\omega(\gamma)\,k_{i2}\right), \\ u(t) &= \Psi(\gamma)_1\alpha(t) + \Psi(\gamma)_2\beta(t) \end{aligned} \tag{19}$$

which is also a particular case for the family of controllers Equation (6).

The next simulations present the behavior of the vehicle with each of the two orientation controllers, Equations (18) and (19), for several initial conditions. The parameters k_{ij} have been adjusted according to the stability results of the above analysis. The desired orientation is $\alpha = \beta = 0$.

Along with the stability conditions proposed in the above analysis, the shape of Ψ_1, Ψ_2 in both controllers has been adjusted to achieve the following conditions:

$$D = 1, \quad \max(\Psi_1) > 5,$$

$$b = \frac{5}{3}, \quad U_{\text{sat}} > \frac{1}{D}.$$

Note from Figure 6 that jackknifing is avoided when using both controllers. Figure 7 shows the simulation of two maneuvers for changing orientation from different initial conditions with the fuzzy orientation controller.

Although the dynamics of the desired η provided by the first level (outer loop) is slow and could be considered as constant, in general the first level will provide a time varying reference according to the desired path. Here, a second analysis with a time varying reference is considered in order to guarantee the behavior of the inner loop orientation control. This is a very general assumption, and a more difficult analysis is required. For this reason, two different references are considered: a *ramp* and a *sine*. These references are very useful in control theory and provide a good idea of the behavior of the system. The analysis makes use of the approximate linearization of the system around the reference. Furthermore, the functions Ψ_1, Ψ_2 will be determined in order to improve the behavior when time-varying references are involved.

Another issue to take into account is that if Equation (7) has to follow a reference $\eta = \eta(t)$, the condition $|\dot{\eta}| < \left(\sin\gamma_{\max}\right)/D$ has to be satisfied. Otherwise, the system will drift from the reference. This can be understood when the speed limitation of β is considered.

Assume that $\eta = \eta(t)$ and

$$\alpha(t) = \bar{\alpha}(t) + \delta\alpha(t) \tag{20}$$

$$\beta(t) = \bar{\beta}(t) + \delta\beta(t) \tag{21}$$

where $\left(\bar{\alpha}(t), \bar{\beta}(t)\right)$ represent the stationary solutions, which are assumed to be in the non-saturation set. Therefore, if we incorporate Equations (20) and (21) into (7) and linearize around the reference, we obtain the following linear time-varying system:

$$\begin{pmatrix} \partial\dot{\alpha} \\ \partial\dot{\beta} \end{pmatrix} = \begin{pmatrix} A_1 & A_2 \\ -\dfrac{\cos(\bar{\gamma})}{D} & \dfrac{\cos(\bar{\gamma})}{D} \end{pmatrix} \begin{pmatrix} \partial\alpha \\ \partial\beta \end{pmatrix}, \tag{22}$$

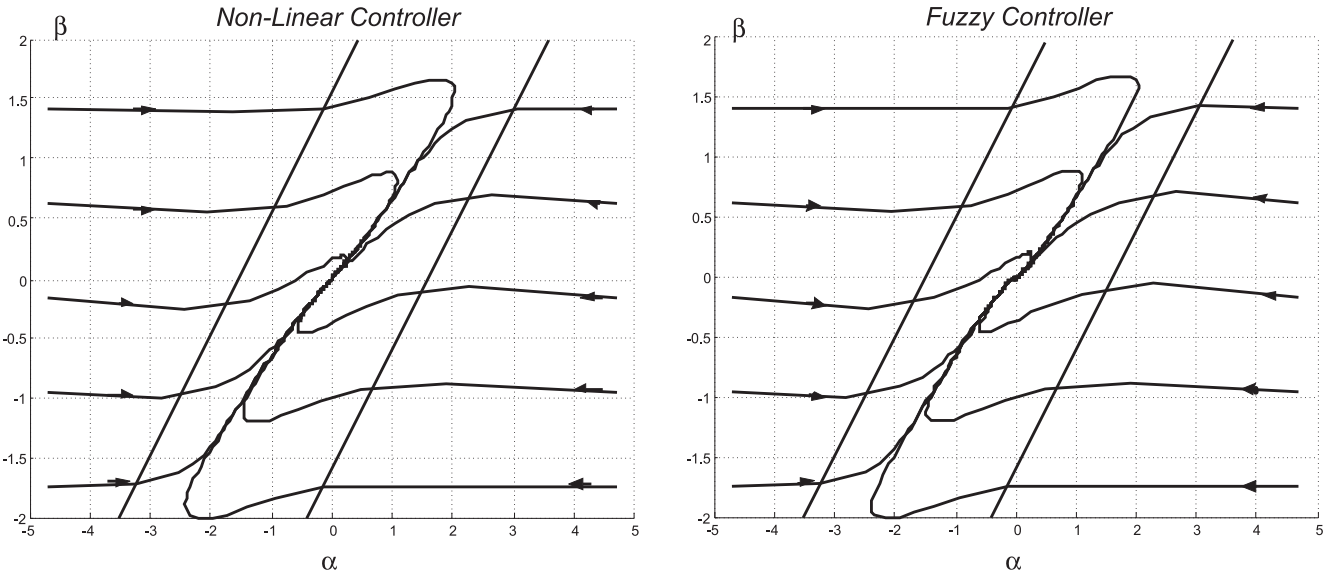

Fig. 6. Simulation of the orientation controllers Equations (18) and (19). The units in the graphics are in radians.

where

$$A_1 = -\Psi_1 - \frac{d\Psi_1}{d\gamma}(\eta - \bar{\alpha}) - \frac{d\Psi_2}{dy}(\eta - \bar{\beta}) \tag{23}$$

$$A_2 = -\Psi_2 + \frac{d\Psi_2}{d\gamma}(\eta - \bar{\alpha}) + \frac{d\Psi_2}{d\gamma}(\eta - \bar{\beta}) \tag{24}$$

when $\bar{\gamma} = \bar{\beta} - \bar{\alpha}$ and $\Psi_i = \Psi(\bar{\gamma})_i$.

1. *Ramp reference*. $\eta = k\tau$. This orientation reference is generated by the pure pursuit strategy at the look-ahead level when the path to be tracked is a circle. It is possible to show that k has to satisfy $|k| < \sin\gamma_{\max}/D$ in order that Equation (7) is able to follow the reference. Otherwise, the system will drift from the reference.

In this case, the stationary solutions can be expressed as:

$$\bar{\alpha} = k\tau + \alpha_0, \quad \bar{\beta} = k\tau + \beta_0. \tag{25}$$

Thus, $\bar{\gamma}_0 = \bar{\beta}_0 - \bar{\alpha}_0$. The stationary solution satisfies

$$k = \frac{\sin\bar{\gamma}}{D} = -\Psi_1\alpha_0 - \Psi_2\beta_0. \tag{26}$$

If we incorporate Equations (25) and (26) into (22), the approximate linearization leads to a constant linear system. Fortunately, the stability of this system is known and depends on the eigenvalues of the Jacobian matrix of Equation (22). If functions Ψ_1, Ψ_2 achieve the previous conditions, it is possible to guarantee the stability for all k. Since the system has two dimensions, the eigenvalues can be characterized by the trace (tr) and the determinant (det) of the Jacobian matrix, which can be expressed as:

$$\mathrm{tr} = -\Psi_1 - \frac{d\Psi_1}{d\gamma}\bar{\gamma} + \frac{\cos\bar{\gamma}}{D} + \frac{\left(\frac{d\Psi_1}{d\gamma} + \frac{d\Psi_2}{d\gamma}\right)(-k + \Psi_1\bar{\gamma})}{\Psi_1 + \Psi_2} \tag{27}$$

$$\det = -\frac{\cos\bar{\gamma}}{D}(\Psi_1 + \Psi_2). \tag{28}$$

According to the previous condition, it is easy to check that $\mathrm{tr} < 0$, $\det > 0, \forall k$, so $\mathrm{Re}\,\lambda_{1,2} < 0, \forall k$.

In order to improve jackknife prevention, another condition on the functions will be included. This condition is intended to prevent overshoot when the system is working near the jackknife position, i.e. $\bar{\gamma} \cong \gamma_{\max}$. Thus, the new condition on Ψ_1, Ψ_2 is:

$$\mathrm{tr}^2 > 4\det. \tag{29}$$

With this condition, the eingenvalue will be real. Therefore, the local stability of the orientation controller when the path is a circle has been shown.

2. *Sine reference* $\eta = \eta_0 \sin(\omega\tau)$, $\eta_0 > 0$. By means of this reference, we intend to study the speed of the system. Since the system is nonlinear, most methods used in the frequency response analysis of linear systems cannot be applied. Furthermore, this is a periodically forced 2D nonlinear system, so the analysis is difficult because it can produce very complex nonlinear behavior such as nonlinear oscillation, torus and chaos.

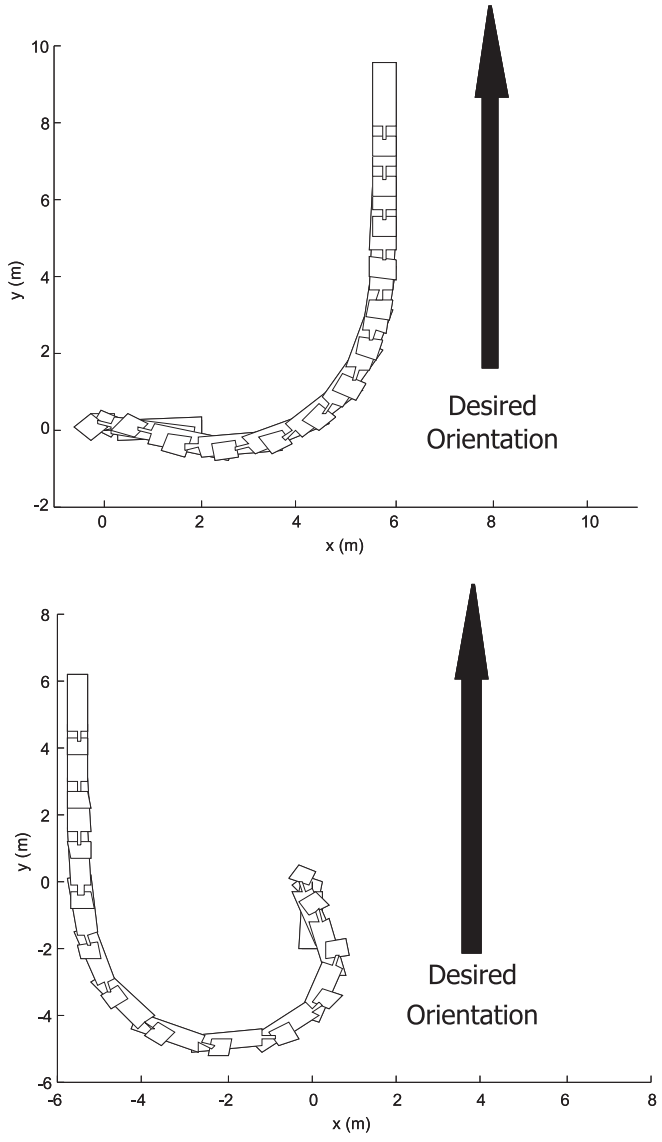

Fig. 7. Simulation of the maneuver.

For example, the forced Duffing oscillator has been studied by many authors who show that it presents several nonlinear behaviors (Lashmanan and Murali 1996).

As mentioned above, although the dynamics behavior of η is slow, the objective of this analysis is to consider time-varying references. Thus, the system with large values of ω will be analyzed.

In the case of $\omega \to 0$, the dynamics of the system is known since η is very slow. Thus, by choosing a small enough value of ω, it is possible to guarantee that α and β will be near η, oscillating and following it. Thus, the system has only one periodic orbit and it is stable. When ω is increased, this orbit can become unstable and the topology can be changed.

The dynamics very near the orbit will be studied here. To this aim, the Poincare map will be used. The Poincare map allows us to detect:

- the change of local stability when ω is varied;
- the appearance of a new periodic orbit by means of the flip and fold bifurcation;
- period-doubling bifurcation of the orbit; and
- the appearance of any torus by means of Neimark-Sacker bifurcation.

In short, we will check that the system continues to follow the sine reference and does not lose control following another orbit. Note that this is a local analysis.

The multipliers of the Jacobian matrix of the Poincare map can be calculated with the variational equation around the orbit. By incorporating $\eta = \eta \sin(\omega t)$ into Equations (22)–(24), the variational equation is therefore obtained, assuming that $\phi(t) = \{\alpha(t), \beta(t)\}$ is the periodic orbit. As the system has two dimensions, there is only one multiplier which is positive and given by:

$$\mu = \exp \int_{-T}^{T} \left(\frac{d\dot{\alpha}}{d\alpha} + \frac{d\dot{\beta}}{d\beta} \right) [\phi(\tau)] \, d\tau, \tag{30}$$

where

$$\frac{d\dot{\alpha}}{d\alpha} = -\Psi_1 - \frac{d\Psi_1}{d\gamma}(\eta - \bar{\alpha}) - \frac{d\Psi_2}{d\gamma}\left(\eta - \bar{\beta}\right) \tag{31}$$

$$\frac{d\dot{\beta}}{d\beta} = \frac{\cos(\bar{\gamma})}{D} \tag{32}$$

are obtained from the variational equation.

As is proved in Appendix B, μ is smaller than 1 for all values of ω. Therefore, the orbit is locally stable and the above-mentioned bifurcations will not appear when ω is varied.

5. Look-Ahead Controller Design

This controller is located in the upper level (outer loop in Figure 4), and its aim is the computation of the desired orientation using the error between the vehicle and a goal point selected at a given look-ahead distance L. This orientation η will be the reference of the orientation reference of the inner loop in Figure 4.

Therefore, as mentioned above, when the dynamics of η is slow enough, the stability of the controllable set is assured. Furthermore, in order to check the operation of the orientation controller, an analysis with different time-varying references was carried out in the above section. This is useful for providing new considerations about Ψ_1 and Ψ_2. The results indicated

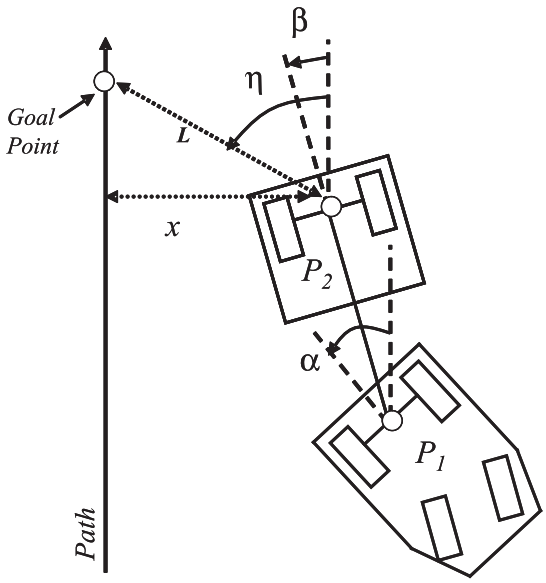

Fig. 8. Line path.

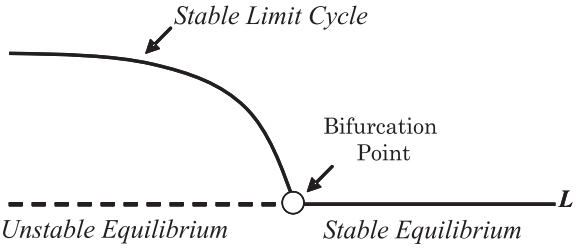

Fig. 9. Bifurcation diagram.

that if the path is smooth, the vehicle will reach the desired orientation. But this result does not necessarily mean that the vehicle will get closer to the path when the look-ahead controller is considered.

Next we will show that if the look-ahead controller is not properly tuned, the vehicle will oscillate even when the path to be followed is smooth. In order to demonstrate this, the tracking of a straight line will be considered. Without any loss of generality of this analysis, it will be assumed that the equation of the line is $x = 0$ (see Figure 8). In this case, the desired orientation can be calculated as follows:

$$\eta(t) = \arcsin \frac{x(t)}{L} \tag{33}$$

where L is the controller's parameter. Next, the qualitative theory of dynamical systems will also be applied for the analysis. Thus, the changes in the equilibrium point, limit cycles and other system behaviors when L is varied will be studied. Then the bifurcation diagram will be represented, allowing an understanding of the global dynamic behavior.

Regarding Equations (2) and (33), the solution to this control problem is $\{\alpha = \beta = x = 0,\ y = v_d t\}$, where v_d is the desired speed. As mentioned in Section 2, the longitudinal control of y by means of v can be achieved in practice with a PID controller and will not be considered here. Thus, the problem consists of the stabilization at the equilibrium point $\{\alpha = \beta = x = 0\}$ by means of the control variable u. Note that α, β and x do not depend on y. This problem involves the consideration of unstable dynamic orientations. The Poincare-Andronov-Hopf theorem (Wiggins 1990) establishes two conditions to guarantee that in the neighborhood of any equilibrium point, the system has a non-trivial periodic orbit. The first condition is that the Jacobian has a pair of eigenvalues and that those eigenvalues cross the imaginary axis with non-zero speed when the bifurcation parameter is varied. It can be shown that if

$$\frac{1}{L} = \Psi(0)_1 - \frac{1}{D}, \tag{34}$$

the Jacobian of the equilibrium point has a pair of eigenvalues which can be expressed as $\lambda = \pm \omega j$, where

$$\omega = \sqrt{\frac{1}{D}\left(\Psi(0)_1 + \Psi(0)_2\right)} \tag{35}$$

and

$$\frac{d}{dL}\mathrm{Re}(\lambda) < 0 \tag{36}$$

at the equilibrium point. Thus, the eigenvalues cross the imaginary axis with non-zero speed.

Finally, the second condition is that the first Lyapunov coefficient should be non-zero. There are several ways to express this coefficient. By using the expression in Wiggins (1990), it is possible to show that the first Lyapunov coefficient is greater than zero. Therefore, a branch of stable periodic orbits emerges from all equilibrium points at Equation (34). Regarding Equation (36), the branch emerges when the value of the parameter L is decreased (see Figure 9).

The system will oscillate if the value of L satisfies the following inequality:

$$\frac{1}{L} > \Psi(0)_1 - \frac{1}{D}. \tag{37}$$

Figures 10 and 11 show an example of a limit cycle. These figures have been obtained by simulating the vehicle with the nonlinear orientation controller proposed above and the look-ahead controller tuned according to Equation (37).

In this situation, the vehicle will oscillate around the path (see Figure 11). Note that even in this situation the orientation controller avoids the jackknife position. Figure 12 shows the simulation of the control system tracking a line path, but in this case L does not satisfy Equation (37). The conclusion of this analysis is that the parameter of the look-ahead controller L has to be greater than the bifurcation point defined in Equation (34).

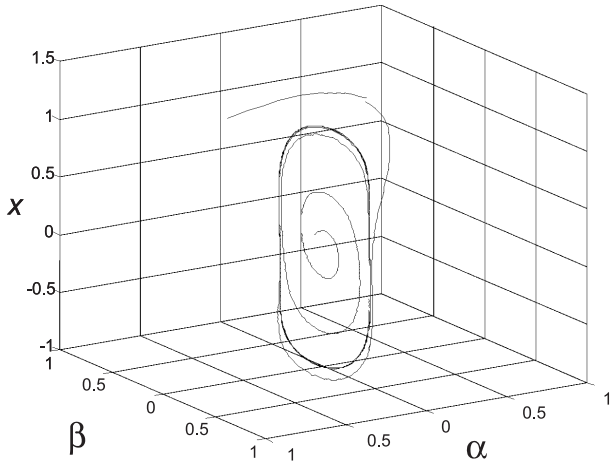

Fig. 10. Limit cycle; the units of the x axis are m, and the units of angles α and β are radians.

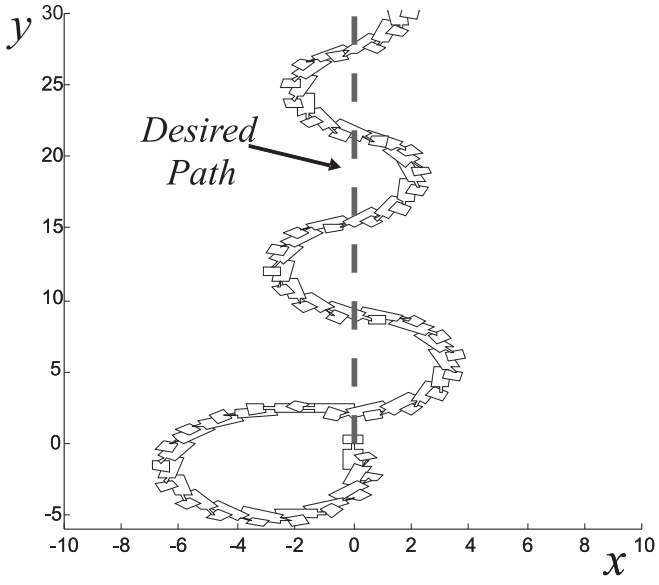

Fig. 11. Oscillation's trajectory (m).

Similar conclusions can be obtained for circular paths. In this case, the system is stable if the truck-trailer will tend to the path. Therefore, the stability analysis has to be applied in the neighborhood of a circular limit cycle. The stability also depends on the look-ahead parameter L. For this problem, the unstable dynamic behavior appears by means of the Neimark-Sacker bifurcation (Wiggins 1990). In this bifurcation, an *invariant torus* bifurcates from the limit cycles. Two conditions are needed for the Neimark-Sacker bifurcation. The first is that the multipliers of the Jacobian around the stable limit cycle are complex and lie on the unit circle. The second condition is that the multipliers cross the unit circle with non-zero speed when

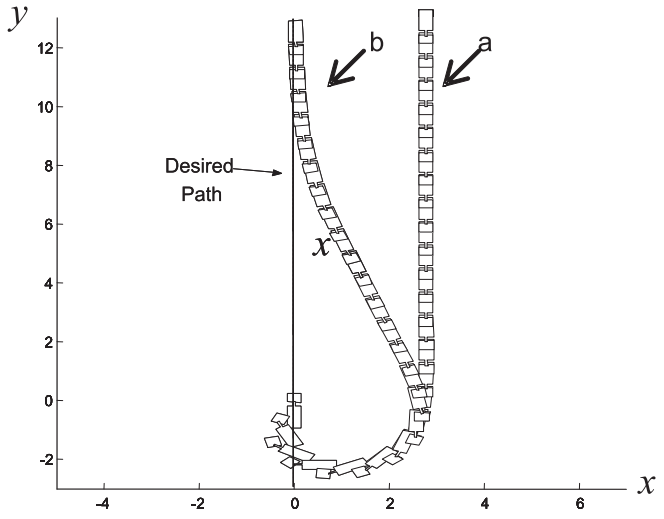

Fig. 12. Line path (m): trajectory obtained (a) when using only the orientation controller; and (b) when the look-ahead and orientation controllers are used.

L is varied. Under these circumstances, this is a global bifurcation and its analysis is very difficult. However, using polar coordinates, it is possible to reduce this problem to a local bifurcation analysis. Then, in the same way as for rectilinear paths, an inequality condition on L can be obtained. It is possible to show that this inequality is less severe than Equation (37). For the sake of brevity, this analysis has been omitted. Figure 13 shows simulations when tracking circle paths.

In conclusion, if L does not satisfies the inequality (37) the look-ahead controller will not oscillate for circular and rectilinear paths.

6. Experimental Results

The proposed controller structure has been implemented in the autonomous Romeo 4R vehicle. The relevance of the maximum allowable curvature and parameter D in the size of the controllable set has been pointed out. In the Romeo 4R (Figure 14) D = 1.9 m and the maximum allowable curvature is very close to $1/D$.

The sensors used in these experiments are:

- two sensors for measuring the position and orientation (a DGPS and a gyroscope);
- two sensors for measuring the speed (an encoder coupled to the tractor rear axle and a Doppler sensor); and
- the angle γ is measured by means of a potentiometer (accuracy 0.037°).

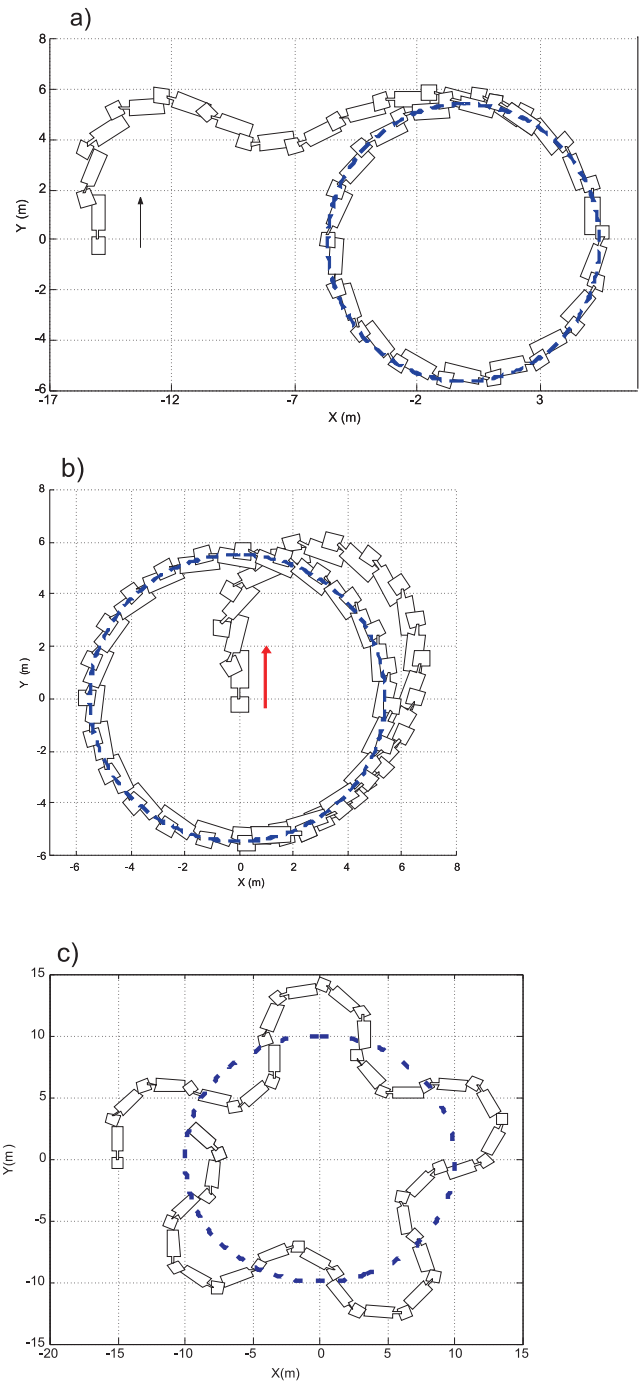

Fig. 13. Tracking of a circle path: (a) and (b) represent a stable limit cycle and (c) represents an unstable cycle; the track-trailer is following a torus.

The Controller is embedded in an industrial PC. The operating system is Debian GNU/Linux 2.2r5 and the software is developed in C++. This controller integrates the following four modules.

Fig. 14. Romeo 4R.

- Trajectory generator: The aim is to give a reference to the look-ahead controller and the PID speed controller. These references are generated depending on the position of the vehicles with respect to the desired trajectory. If the vehicle diverts from the desired trajectory in a significant distance, the generator will generate a virtual trajectory that will converge to the desired trajectory.
- Look-ahead controller.
- Orientation controller.
- Position/Orientation estimation. This module integrates the measurements from all the different sensors and estimates the position and the orientation. These estimations are used by the controllers.

The actuator comprises two DC Motors for steering and velocity command controlled by two PIDs. These PIDs are integrated in a motion control card.

Figure 15 shows the architecture of the control system. It should be noted that the position and orientation estimation mentioned above are obtained by means of sensor data fusion techniques that are not described in this paper. These techniques have demonstrated robustness to sensor noise and model uncertainties (see Rodriguez- Castaño 2008).

According to the Controllability Minimum Principle, the controllable set of the Romeo 4R is given by $|\gamma| \leq \pi/2$. The analysis in previous sections is based on a 2D kinematics model for planar motions in compact terrain and does not consider the vehicle-terrain interactions and the actuator dynamic behavior. Both are common assumptions in vehicles moving at low velocity in flat terrain as is the case of the experiments that will be described in this section. Particularly, if the dynamic behavior of the actuator is fast with respect to the vehicle's velocity, the effect of this dynamic behavior can be neglected. However, if the actuator is slow (i.e. due to the mechanical transmission, the constants of the PID orientation controller or

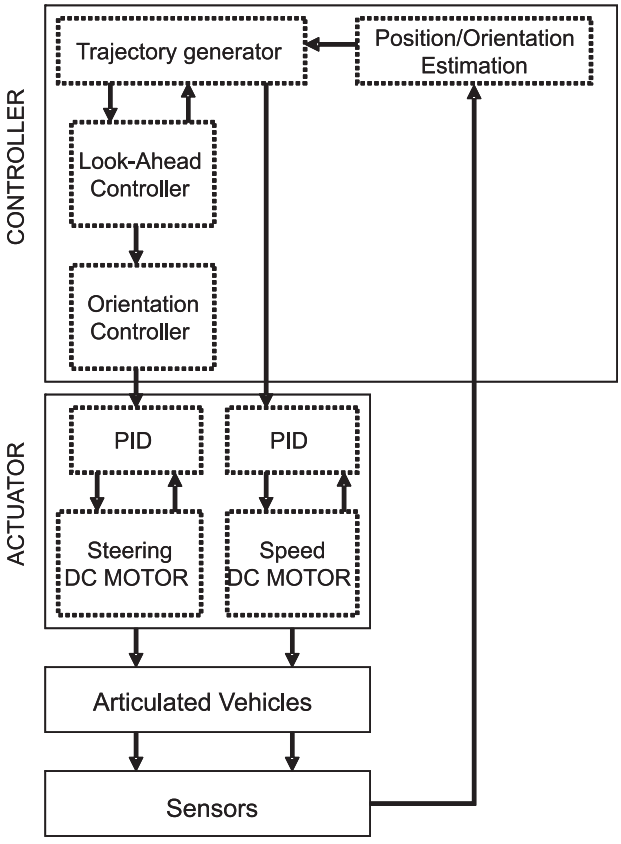

Fig. 15. Architecture of the control system.

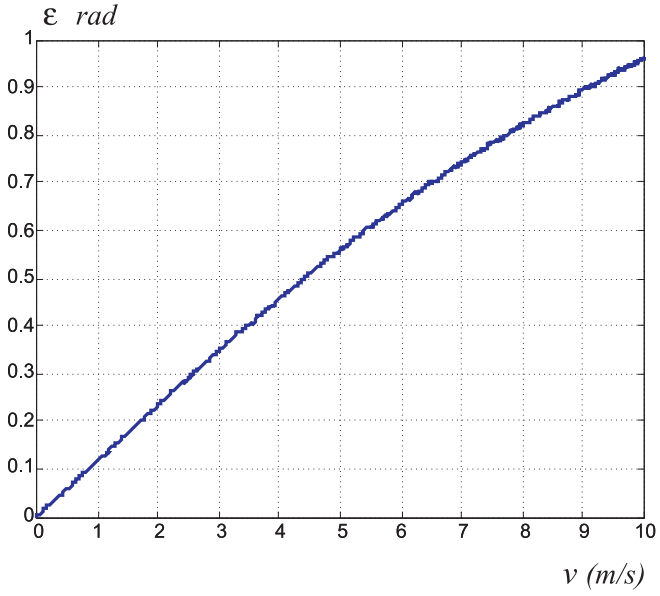

Fig. 16. Controllable set for different values of v.

the torque saturation), the controllable set computed in previous sections should be decreased. For the particular case of the Romeo 4R autonomous vehicle, the steering actuator of the vehicle can be modeled as a first-order linear system with a time constant 0.2 s (see Rodriguez-Castaño 2008).

By using the Controllability Minimum Principle in Section 3, it can be shown that the controllable set is given by $|\gamma| \leq \pi/2 - \varepsilon$, where $\varepsilon > 0$ and depends on v, as shown in Figure 16. The curve in this figure has been computed by applying the controllability principle. First, a point on the border of the controllability region is computed. Specifically, the point given by $\gamma_{\max} = +\arcsin(DU_{\text{sat}})$ is computed. At this point, $\dot{\gamma} \geq 0$. Then, the backward integration of the full model (1) is performed with $u = -U_{\text{sat}}$ until the real maximum curvature (output of the above mentioned linear control system) of the tractor U_{sat} is obtained. The value of the curvature in this position is $\gamma = \bar{\gamma}$; then $\varepsilon = \gamma_{\max} - \bar{\gamma}$.

The maximum velocity of Romeo 4R for backward maneuvers is $v = 1$ m s^{-1}. Thus, $\varepsilon < 0.13$ and the effect on the controllability set can be neglected, which is not the case for higher velocities of the vehicle (see Figure 16).

Thus, it can be concluded that for the Romeo 4R vehicle navigating backward in flat terrain, the assumptions and models in the previous sections are valid and the analysis for avoiding the jackknife condition can be applied. Furthermore, in order to compensate for the approximation errors due to the dynamics and the vehicle–terrain interaction, the controller is designed with $\gamma_{\max} = 1.2$ to increase the robustness in order to avoid the jackknife condition.

The experimental results were obtained with the nonlinear controller proposed in
Equation (18). Similar results were obtained with another orientation controller with Equation (6).

Two types of experimental results will be presented below. The first type shows the dynamics of the orientation controller when a desired orientation is set. The second shows the vehicle's behavior when a general path is tracked and the two levels of the control system in Figure 4 are working.

6.1. Orientation Controller Experiments

As was indicated, the objective of this controller is that the vehicle follows the desired orientation η, avoiding loss of control and therefore the jackknife position. Figure 17 shows the dynamics behavior of β and γ when the orientation controller Equation (18) is implemented and the desired orientation is $\eta = 0$. The controller parameters are $k_{11} = 0.6$; $k_{12} = 0.2$; $k_{21} = -0.6$; $k_{22} = 0$ in Equation (18), and the initial condition is $\langle \beta(0), \gamma(0) \rangle = \langle -180, 0 \rangle$. Note that in practice the system does not exactly reach the desired orientation because of a small oscillation caused by the error in the γ sensor and floor surface irregularities. Furthermore, it should be noted that the jackknife position is avoided throughout the whole maneuver.

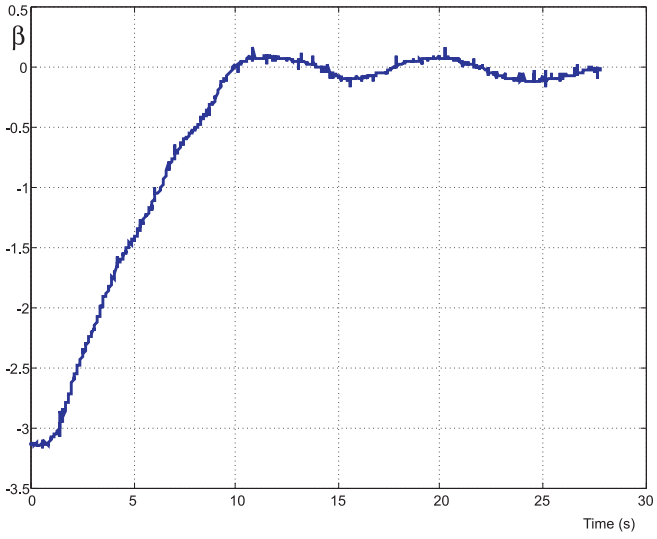

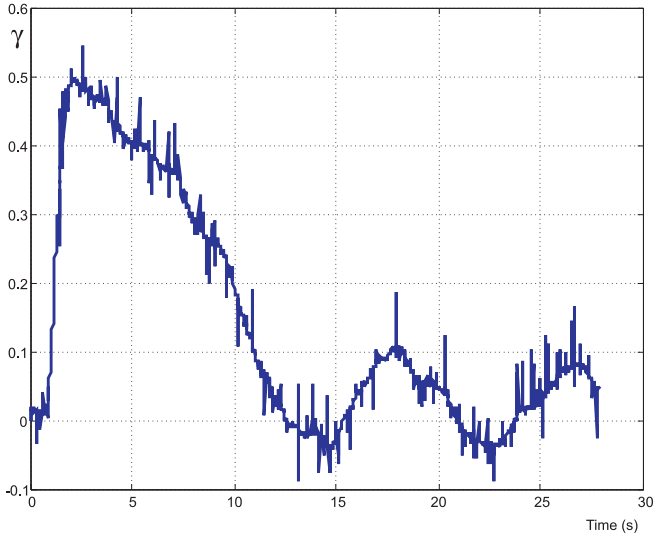

Fig. 17. Dynamic behavior of β and γ (radians).

Thus, the experimental results are in agreement with the analysis.

Another issue that should be noted here is that if the parameters are changed to make the dynamics faster, the vehicle needs larger values of γ. This should be considered to avoid the jackknife position. In this example the maximum value was 0.5.

6.2. General Path Tracking

Next, a general path tracking will be shown. The same orientation controller used in the experiment above was implemented.

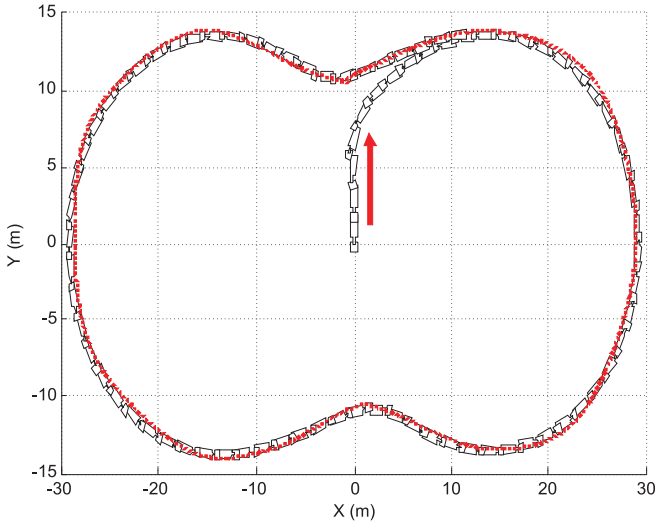

Fig. 18. Real pursuit with Romeo 4R (m).

A pure pursuit controller with a look-ahead L= 5 m was implemented in the second level (the outer loop in Figure 4). Figure 18 shows the results when tracking a closed path.

The tracking results are very good. The maximum deviation with respect to the desired path was 0.2 m. Similar results were obtained with other paths.

7. Conclusions

Stability analysis is an important issue in the maneuvering of tractor-trailer vehicles. This paper has presented a wide family of control systems for backing-up maneuvers and the corresponding stability analysis. The analysis highlighted some conditions for improving the design of the controller. The design of a control system to prevent jackknifing and loss of control has been studied. The saturation of the actuator, frequently encountered in practice, and the related controllability problem were considered in the analysis and design of the control system.

The paper proposes a general control law for the orientation controller and the conditions to guarantee stability in this general control law, which can be particularized for different control strategies including nonlinear controllers with an additive structure in the tractor and trailer orientation errors and fuzzy control. The orientation controller is the lower control level (inner loop) in a structure in which the higher control level for tracking the path backward is a look-ahead controller. The application of the qualitative theory of nonlinear dynamical systems is applied to guarantee the stability of the proposed control system.

A similar procedure can be applied when the joint linking the trailer to the tractor is not located at the midpoint of the

tractor rear axis. Note that, just as with an on-axle hitching model, the saturation can cause an uncontrollability region. Therefore, a similar control structure can be applied.

The experiments with the autonomous Romeo 4R tractor-trailer vehicle have validated the proposed methods. Thus, both the designed orientation controller and general path tracker provided good results when implemented in the Romeo 4R.

Future work will include the integration of this type of controller in a fully autonomous tractor-trailer navigation system including perception, path planning and reactive components. Moreover, the results can also be used to provide autonomous functions for conventional manned vehicles. These driving aids could be helpful when maneuvering in complex environments requiring significant driver ability.

Acknowledgements

This research has been partially funded by the AEROSENS (DPI2005-02293. 2005-2008) and CROMAT (DPI2002-04401-C03-03) projects of the Spanish *Dirección General de Investigación*. The assistance of researchers and technicians from the *Grupo de Robótica Visión y Control* for the experiments presented in the paper is acknowledged. The authors also acknowledge the corrections and comments of the anonymous reviewers, which have been useful for significantly improving the paper.

Appendix A

The objective of this appendix is to prove that system (7) does not have a limit-cycle. Let Φ^1, Φ^{-1}, Ω^{-1} and Ω^1 be sets defined as follows:

$$\Phi^1 = \left\{\alpha, \beta / \left(\dot{\alpha}, \dot{\beta}\right) \nabla \left(\Psi_1\alpha + \Psi_2\beta\right)^T > 0\right\} \quad (38)$$

$$\Phi^{-1} = \left\{\alpha, \beta / \left(\dot{\alpha}, \dot{\beta}\right) \nabla \left(\Psi_1\alpha + \Psi_2\beta\right)^T < 0\right\} \quad (39)$$

$$\Omega^1 = \left\{\alpha, \beta \in S^1 \cap \Phi^1\right\} \quad (40)$$

$$\Omega^{-1} = \left\{\alpha, \beta \in S^{-1} \cap \Phi^{-1}\right\}. \quad (41)$$

Proposition 2: *If* Π *is a limit-cycle of system* (7)*, it has to cross* S^1 *and* S^{-1} *with* $\alpha < 0$ *and* $\alpha > 0$*,* respectively.

Proof: All trajectories that enter S^1 have to do so through Ω^1 since $\tilde{N}\left(\Psi_1\alpha + \Psi_1\beta\right)^T$. In addition to this fact, $\alpha < 0$ in set Ω^1 and $\dot{\alpha} < 0$ in set S^1, so the limit cycle crosses S^1 with $\alpha < 0$. Similar reasoning can be applied in the case of S^{-1}.

Proposition 3: *If* Π *is a limit-cycle of the system* (7) *and* $P = \left(\alpha_0, \beta_0\right)$ *is a point of* Π *with* $\beta_0 = 0$*, then this point has to belong to* S^0.

Proof: Assume that $\alpha_0 > 0$. Since $\Psi_1 > 0, \forall\gamma$, the point cannot belong to S^{-1}. Moreover, taking into account Proposition 2, it has to belong to S^0. Similar reasoning can be applied in case of $\alpha_0 > 0$.

According to the above propositions, the Lyapunov-function (8) evaluated in $\Lambda = \left\{\alpha, \beta/\beta = 0 \cap S^0\right\}$, is smaller than the minimum value evaluated in Ω^1 or Ω^{-1}. This will be shown below in order to prove that there is no limit cycle.

The maximum value of the Lyapunov-function (8) evaluated in Λ corresponds to the maximum value of $\alpha \in \Lambda$.

$$\max_{\alpha,\beta\in\Lambda} V = \alpha_{\max}^2 = \left(\frac{U_{\text{sat}}}{\Psi_1}\right)^2 < \left(b\frac{U_{\text{sat}}}{\min\Psi_2}\right)^2. \quad (42)$$

The computation of the minimum value of the Lyapunov-function (8) evaluated in Ω^1 or Ω^{-1} is more difficult because Ψ_1 and Ψ_2 are not defined. However, it can be bounded by using the following set:

$$\Omega' = \{\alpha, \beta / \min\Psi_1\alpha + \min\Psi_2\beta = U_{\text{sat}}, \beta < \alpha < 0\}. \quad (43)$$

It is easy to show that the minimum value of the Lyapunov-function (8) in Ω' is smaller than the minimum in Ω^1 or Ω^{-1}. Thus, the minimum of Ω' is a lower bound of the minimum of Ω^1 and Ω^{-1}.

Differentiating the Lyapunov-function (8) and taking into account Equation (43),

$$\left.\frac{dV}{d\beta}\right|_{\Omega'} > 0. \quad (44)$$

The minimum value corresponds to

$$\alpha = 0, \quad \beta = \frac{U_{\text{sat}}}{\Psi_2},$$

so

$$\min_{\alpha,\beta\in\Omega'} V = a\left(\frac{U_{\text{sat}}}{\Psi_2}\right)^2 > a\left(\frac{U_{\text{sat}}}{\min\Psi_2}\right)^2. \quad (45)$$

If $a > b^2$ the trajectories that go through Λ will not enter S^1 or S^{-1} because $\dot{V} < 0, \forall\alpha, \beta \in S^0$. Therefore, system (7) does not have a limit-cycle.

Appendix B

The objective of this appendix is to show some properties which are useful for the controller design.

Proposition 4: *Let*

$$\dot{x} = f(x,t) + g(x), x \in R^n \quad (46)$$

be a 2T-periodically forced system where $f(x,t)$ *and* $g(x)$ *are* C^r $(r \geq 1)$ *and:*

- $f(x,t) = f(x,-t)$
- $f(x,t+T) = -f(x,t)$
- $g(x) = g(-x)$

Let $\phi(t), \Phi \in R^n$ be a 2T-periodic orbit of the system (46); then:

$$\phi(t+T) = -\phi(t). \tag{47}$$

Proof: Since $\phi(t+T)$ is a solution (Wiggins 1990), the next relationship has to be achieved:

$$\begin{aligned}\frac{d\phi(t+T)}{dt} &= f(t+T,\phi(t+T)) + g(\phi(t+T)) \\ &= -f(t,\phi(t+T)) + g(\phi(t+T)).\end{aligned} \tag{48}$$

Based on Equation (47), the above relation can be expressed as:

$$-\frac{d\phi(t)}{dt} = -f(t,\phi(t)) - g(\phi(t)). \tag{49}$$

Taking into account that $\phi(t)$ is a solution, the above relationship is satisfied. Since the solution in a vector field Equation (46) is unique, the proposition is proved.

Notice that when the orientation reference is $\eta = \eta_0 \sin(\omega\tau)$, system (7) has the same structure as system (46), where

$$f = \begin{pmatrix} \Psi_1 \eta(\tau) + \Psi_1 \eta(\tau) \\ 0 \end{pmatrix} \tag{50}$$

$$g = \begin{pmatrix} \Psi_1(-\alpha) + \Psi_1(-\beta) \\ \dfrac{\sin\gamma}{D} \end{pmatrix}. \tag{51}$$

Therefore, if $\phi(\tau) = \{\bar{\alpha}(\tau), \bar{\beta}(\tau)\}$ is a 2T-periodic orbit, the following relationship has to be satisfied:

$$\int_{-T}^{T} \bar{\alpha}(\tau)d\tau = 0, \quad \int_{-T}^{T} \bar{\beta}(\tau)d\tau = 0. \tag{52}$$

Similar reasoning can be applied to $\bar{\gamma}$.

Taking into account the above result, it will be shown that the multiplier given by Equation (30) is smaller than 1 when ω is increased. That is:

$$\int_{-T}^{T} \left(\frac{d\dot{\alpha}}{d\alpha} + \frac{d\dot{\beta}}{d\beta}\right)[\phi(\tau)]\,d\tau < 0. \tag{53}$$

If we insert Equations (31) and (32) into (53), we obtain:

$$\int_{-T}^{T} \left(-\Psi_1 + \frac{\cos\bar{\gamma}}{D} - \frac{d\Psi_1}{d\gamma}\bar{\gamma} + \left(\frac{d\Psi_1}{d\gamma} + \frac{\Psi_1}{d\gamma}\right)(\bar{\beta} - \eta)\right) d\tau. \tag{54}$$

In order to calculate the above integral, the time origin $\bar{\gamma}(0) = 0$ is chosen. As λ crosses zero twice, the origin of τ will be chosen when $\bar{\gamma}(0) > 0$. However $\bar{\gamma}$ is an odd function, i.e.

$$\int_{-\tau}^{\tau} \overline{\gamma}(\tau)\,d\tau = 0, \forall\tau. \tag{55}$$

Therefore, $\bar{\gamma}$ can be expressed using the Fourier series as follows:

$$\bar{\gamma}(\tau) = \sum_{i=1}^{\omega} \gamma_n \sin(n\omega\tau) \tag{56}$$

with $\gamma_1 > 0$. Furthermore, as $\Psi(\gamma)_{1,2} = \Psi(-\gamma)_{1,2}$,

$$\int_{-T}^{T} \frac{d\Psi_1}{d\gamma}(\tau)\,d\tau = 0, \quad \int_{-T}^{T} \frac{d\Psi_1}{d\gamma}(\tau)\,d\tau = 0, \forall\tau. \tag{57}$$

$\dfrac{d\Psi_1}{d\gamma}$ and $\dfrac{d\Psi 2}{d\gamma}$ are odd functions.

This property will be very useful for calculating Equation (54), as will be seen. Due to the complexity of the integral, it is broken down into different terms to make the proof easier. It will be shown that each term of Equation (54) is equal to or less than zero. Regarding the first element, since $\Psi_1 > 1/D$, it is less than zero, i.e.

$$\int_{-T}^{T} \left(-\Psi_1 + \frac{\cos\bar{\gamma}}{D}\right) d\tau < 0 \tag{58}$$

Since $\dfrac{d\Psi_1}{d\gamma}$ and $\bar{\gamma}$ have the same sign,

$$-\int_{-T}^{T} \frac{d\Psi_1}{d\gamma}\bar{\gamma}\,d\tau < 0, \tag{59}$$

where the second term is less than zero. The last term is the most difficult to study. It has therefore been divided as follows:

$$\int_{-T}^{T} \left(\frac{d\Psi_1}{d\gamma} + \frac{d\Psi_2}{d\gamma}\right)\bar{\beta}d\tau - \int_{-T}^{T} \left(\frac{d\Psi_1}{d\gamma} + \frac{d\Psi_2}{d\gamma}\right)\eta d\tau. \tag{60}$$

Taking into account Equation (7), $\bar{\beta}(\tau)$ is an even function and the first integral is zero. The second integral of Equation

(60) is less than zero. In order to show this, the *Fourier series expansion* has been used. Thus, the following decompositions will be used

$$\frac{d\Psi_1}{d\gamma} = \sum_{i=1}^{\infty} \Psi'_{1n} \sin n\omega\tau \tag{61}$$

$$\frac{d\Psi_2}{d\gamma} = \sum_{i=1}^{\infty} \Psi'_{2n} \sin n\omega\tau \quad \Psi_1 = \sum_{i=0} \Psi_{1n} \cos n\omega\tau \tag{62}$$

$$\Psi_2 = \sum_{i=0}^{\infty} \Psi_{2n} n \cos n\omega\tau \quad \bar{\beta} = \sum_{i=0}^{\infty} \beta_n \cos n\omega\tau \tag{63}$$

where the following relationships are satisfied:

- $\Psi'_{1n} > 0$, $\Psi'_{2n} < 0$ and $\Psi'_{1n} + \Psi'_{2n} > 0$;
- $\Psi_{10} > 0$, $\Psi_{20} < 0$ and $\Psi_{10} + \Psi_{20} < 0$; and
- $\beta_0 = 0$.

Thus,

$$\begin{aligned} &- \int_{-T}^{T} \left(\frac{d\Psi_1}{d\gamma} + \frac{d\Psi_1}{d\gamma} \right) \eta d\tau \\ &= - \int_{-T}^{T} \sum_{i=1}^{\infty} \left(\Psi'_{1i} + \Psi'_{2i} \right) \sin\left(n\omega\tau\right) \cdot \eta_0 \sin\left(\omega\tau + \phi\right) d\tau \\ &- \left(\Psi'_{11} + \Psi'_{21} \right) \eta_0 \cos\phi \cdot T \end{aligned} \tag{64}$$

where ϕ is the phase shift of η due to the new time origin.

The next step is to determine ϕ. To this aim, the first-harmonic balance has been applied in

$$\dot{\gamma} = \frac{\sin\gamma}{D} + \left(\Psi_1 + \Psi_2\right)\eta + \Psi_1\left(\gamma - \beta\right) + \Psi_2\beta. \tag{65}$$

Thus, we obtain:

$$\begin{aligned} 0 &= \frac{N}{D} - \left(\Psi_{10} + \Psi_{20}\right)\eta_0 \cos\phi - \Psi_{10}\gamma_1 \\ \gamma_1 \omega j &= -\left(\Psi_{10} + \Psi_{20}\right)\eta_0 \sin\phi \cdot j \\ &+ \left(-\Psi_{10} + \Psi_{20}\right)\beta_0 \cdot j \end{aligned} \tag{66}$$

where

$$N = \frac{1}{\pi} \int_{-\pi}^{\pi} \sin\left(\bar{\gamma}\right) \sin\left(\omega t\right) d\left(\omega t\right). \tag{67}$$

Using the above equation, it is possible to get

$$\cos\phi = \frac{\Psi_{10}\gamma_1 - N/D}{-\left(\Psi_{10} + \Psi_{20}\right)\eta_0} > 0. \tag{68}$$

Therefore, Equation (64) is smaller than zero and the multiplier given by Equation (30) is smaller than one.

References

Amidi, O. (1990). Integrated Mobile Robot Control. Carnegie Mellon University Robotics Institute, Technical Report CMU-RI-TR-90-17.

Altafini, C., Speranzon, A. and Wahlberg, B. (2001). A Feedback Control Sheme for Reversing a Truck and Trailer Vehicle. In *IEEE Transactions on Robotic and Automation* **17**(6): 915–922.

Astolfi, A., Bolzern, P. and Locatelli, A. (2004). Path-tracking of a tractor-trailer vehicle along rectilinear and circular paths: a Lyapunov-based approach. In *IEEE Transactions on Robotic and Automation* **20**(1): 154–160.

Bolzern, P. and Locatelli A. (2002). A comparative study of different solutions to the path-tracking problem for an articulated vehicle. In Proceedings of the 2002 International Conference on Control Applications, Glasgow, Scotland, UK, pp. 427–434.

De Luca, A., Oriolo, G. and Samson, C. (1998). Feedback control of a nonholonomic car-like robot. *Robot Motion Planning and Control*, J. P. Laumont (ed.), London, Springer-Verlag, pp. 171–253.

DeSantis, R. 1994. Path tracking for a tractor-trailer-like robot. *International Journal of Robotics Research* **13**(6): 533–544.

González-Cantos, A., Maza, J.I. and Ollero, A. (2001). Design of a stable backing up fuzzy control of autonomous articulated vehicles for factory automation. Proceedings of the *IEEE International Conference on Emerging Technologies and Factory Automation*, Antibes-Juan Lespins, France.

Kim, D.H. and Oh, J.H. (1999). Experiments of backward tracking control for trailer systems. In *Proceedings of the 1999 International Conference on Robotics and Automation*, Detroit, MI, USA, vol **1**, pp 19–22.

Kong, S. and Kosko, B. (1992). Adaptative Fuzzy System for Backing up and Truck-and-Trailer. *IEEE Transactions on Neural Networks* **3**(3): 211–223.

Lamiraux, F. and Laumond, J.P. (1998). A practical approach to feedback control of a mobile robot with trailer. In *Proceedings of 1998 International Conference on Robotics and Automation*, Leuven, Belgium, pp 3291–3296.

Lamiraux, F., Sekhavat, S. and Laumond, J.P. (1999). Motion planning and control for Hilare pulling a trailer. *Robotics and Automation* **15**(4): 640–653.

Lashmanan, M. and Murali, K. (1996). *Chaos in Non-linear Oscillations*. World Scientific, Singapore.

Li W., Tsubouchi, T. and Yuta, S. (1999). On a manipulative difficulty of a mobile robot with multiple trailers for pushing and towing. In *Proceedings of 1999 International Conference on Robotics and Automation*, Detroit, MI, vol. **1**, pp 13–18.

Nakamura, Y., Ezaki, H., Tan, Y. and Cheng, W. (2000). Design of steering mechanism and control of nonholonomic trailer systems. In *Proceedings of 2000 International Con-*

ference on Robotics and Automation, San Francisco, CA, vol. **1**, pp 247–254.

Rodriguez-Castaño, A. (2008). Position estimation and control of autonomous vehicles at high speed (in Spanish). PhD Dissertation. University of Seville, Spain.

Sampei, M, Tamura, T., Kobayashi, T. and Shibui, H. (1995). Arbitrary path-tracking control of articulated vehicles using nonlinear control theory. *IEEE Transactions on Control Systems Technology* **3**: 125–131.

Samson, C. (1995). Control and Chained Systems. Application to Path Following and Time–Varing Point-Stabilization of Mobile Robots. *IEEE Transactions on Automatic Control* **40**(1): 64–77.

Tanaka, K. and Sano, M. (1994). A robust stabilization problem of fuzzy control systems and its application to backing up control of a truck-trailer. In *IEEE Transactions on Fuzzy Systems* **2**: 119–133.

Tanaka, K. and Kosaki, T. (1997). Design of Stable Fuzzy Controller for an Articulated Vehicle. In *IEEE Transactions on Systems*, *Man, and Cybernetics, Part B: Cybernetics* **27**(3): 552–558.

Thomas, L. and Walter, J. (1997). *Non Linear and Optimal Control Systems*. New York, NY, John Wiley & Sons, Inc.

Tokunaga, M. and Ichihashi, H. (1992). Backer-upper control of a trailer truck by neuro-fuzzy optimal control. In *Proceedings of 8th Fuzzy System Symposium*, Hiroshima, Japan, pp. 49–52 (in Japanese).

Wiggins S. (1990). *Introduction to Applied Nonlinear Dynamical Systems and Chaos*. London, UK, Springer-Verlag.